Elevated glucose inhibits VEGF-A–mediated endocardial cushion formation: modulation by PECAM-1 and MMP-2

Josephine M. Enciso,[1,2] Dita Gratzinger,[1] Todd D. Camenisch,[3,4] Sandra Canosa,[1] Emese Pinter,[1,2] and Joseph A. Madri[1]

[1]Department of Pathology and [2]Department of Pediatrics, Yale University School of Medicine, New Haven, CT 06520
[3]College of Pharmacy, University of Arizona, Tucson, AZ 85721
[4]Steele Memorial Children's Research Center, College of Medicine, University of Arizona, Tucson, AZ 85724

The Journal of Cell Biology

Atrioventricular (AV) septal defects resulting from aberrant endocardial cushion (EC) formation are observed at increased rates in infants of diabetic mothers. EC formation occurs via an epithelial-mesenchymal transformation (EMT), involving transformation of endocardial cells into mesenchymal cells, migration, and invasion into extracellular matrix. Here, we report that elevated glucose inhibits EMT by reducing myocardial vascular endothelial growth factor A (VEGF-A). This effect is reversed with exogenous recombinant mouse VEGF-A$_{165}$, whereas addition of soluble VEGF receptor-1 blocks EMT. We show that disruption of EMT is associated with persistence of platelet endothelial cell adhesion molecule-1 (PECAM-1) and decreased matrix metalloproteinase-2 (MMP-2) expression.

These findings correlate with retention of a nontransformed endocardial sheet and lack of invasion. The MMP inhibitor GM6001 blocks invasion, whereas explants from PECAM-1 deficient mice exhibit MMP-2 induction and normal EMT in high glucose. PECAM-1–negative endothelial cells are highly motile and express more MMP-2 than do PECAM-1–positive endothelial cells. During EMT, loss of PECAM-1 similarly promotes single cell motility and MMP-2 expression. Our findings suggest that high glucose-induced inhibition of AV cushion morphogenesis results from decreased myocardial VEGF-A expression and is, in part, mediated by persistent endocardial cell PECAM-1 expression and failure to up-regulate MMP-2 expression.

Introduction

Infants born to mothers with gestational diabetes have a threefold increased risk of cardiovascular malformations (Boughman et al., 1993). Defects resulting from aberrant endocardial cushion (EC)* formation, such as atrioventricular (AV) septal defects, are strongly associated with maternal diabetes (Loffredo et al., 2001). The nature of these defects indicates that poor glycemic control during early stages of cardiac morphogenesis has significant teratogenic effects via molecular mechanisms that remain undefined.

The ECs are precursors of the AV valves and a portion of the AV septum. EC formation occurs via an epithelial-mesenchymal transformation (EMT) in which a subpopulation of endothelial cells within the endocardial layer adjacent to the atrioventricular canal (AVC) down-regulate cell adhesion molecules (Mjaatvedt and Markwald, 1989), separate from the endocardium, and transform into migratory mesenchymal cells that invade into the underlying cardiac jelly (Runyan and Markwald, 1983). The development of in vitro chick and mouse models of EC development has greatly advanced our understanding of the cellular events and molecular regulation of EMT. AVC explants cultured on three-dimensional collagen gels according to the method of Bernanke and Markwald (1979) recapitulate the in vivo process of EMT. This assay has been used to demonstrate that EMT involves multiple steps initiated by inductive signals from the myocardium in a permissive ECM en-
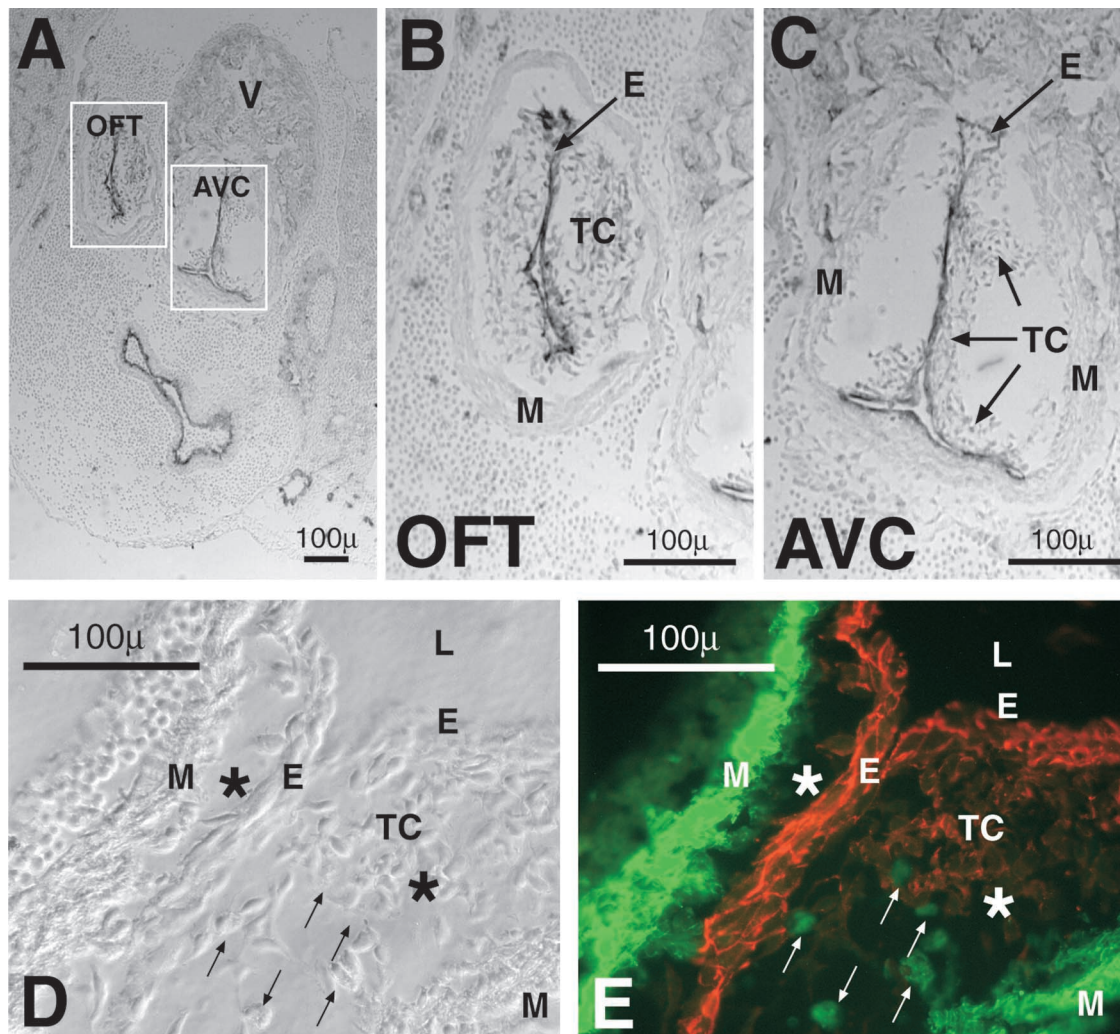
Figure 1.   **PECAM-1 expression is lost as endocardial cells undergo EMT.** Peroxidase (A–C) and phase/fluorescence (D and E) microscopic images of the cardiac region at 9.5 dpc demonstrating localization of PECAM-1 (red) and α-SMA (green). A illustrates the atrioventricular canal (AVC), ventricle (V), and a cross section of the outflow tract (OFT). OFT (B) and AVC (C) are high power images of the boxed areas in A, showing the outflow tract (OFT) and atrioventricular canal (AVC) comprised of intensely staining PECAM-1–positive endocardial cells (E) lining the lumen, an investing myocardial layer (M), and the intervening cardiac jelly containing transformed endocardial cells (TC) that have lost PECAM-1 staining and have undergone EMT. D is a high power phase-contrast image of an area of EMT. L is the lumen; E denotes the endocardial layer; M denotes the myocardial layer; asterisk denotes the cardiac jelly; TC denotes transformed mesenchymal cells that have dissociated from the endocardial layer and have migrated into the cardiac jelly. The small arrows denote transformed mesenchymal cells that have lost PECAM-1 expression and are expressing α-SMA (panel E). E is a high power immunofluorescence image of the same area of EMT. The endocardial lining is PECAM-1–positive (red). The cardiac jelly (asterisk) has been infiltrated by transformed mesenchymal cells (TC) that have lost most of their PECAM-1 expression and others that have acquired α-SMA expression (green; indicated by small white arrows). L, lumen. Bars, 100 μm.

vironment (Krug et al., 1985, 1987; Ramsdell and Markwald, 1997). EMT is further regulated by multiple transcription factors, growth factors, adhesion molecules, and proteases (Lee et al., 1995; Erickson et al., 1997; Boyer et al., 1999a,b; Camenisch et al., 2000, 2002b; Nakajima et al., 2000; Song et al., 2000; Boyer and Runyan, 2001; Dor et al., 2001).

Inhibition of EC formation has been shown to occur in embryos from streptozotocin-induced diabetic mice and in murine embryos cultured in hyperglycemic conditions (Pinter et al., 1999). In the embryonic yolk sac, hyperglycemia elicits an arrest in yolk sac vasculogenesis that correlates with a reduction in VEGF-A mRNA and protein levels (Pinter et al., 2001). VEGF-A is an indispensable modulator of cardiovascular development, and both modest increases and decreases in VEGF-A levels in the yolk sac and heart lead to embryonic lethality (Carmeliet et al., 1996; Miquerol et al., 2000; Damert et al., 2002). There is evidence to suggest that maintenance of appropriate VEGF-A levels is important during AVC morphogenesis (Dor et al., 2001). It was demonstrated that hypoxia-driven elevations in VEGF-A and exogenous VEGF-A blocked EMT. Hyperglycemia, like hypoxia, can lead to increased VEGF-A production in adult vascular cells (Natarajan et al., 1997); however, in the developing conceptus, reductions in VEGF-A occur in response to hyperglycemia and correlate with significant vascular abnormalities (Pinter et al., 2001).

Previously, we demonstrated that high glucose results in changes in platelet endothelial call adhesion molecule-1 (PECAM-1) phosphorylation during aberrant vasculogenesis in the yolk sac (Pinter et al., 1999; Ilan et al., 2000). PECAM-1 is a 130-kD member of the immunoglobulin superfamily that modulates cell adhesion, endothelial cell migration, and in vitro and in vivo angiogenesis (Schimmenti et al., 1992; Lu et al., 1996, 1997; DeLisser et al., 1997; Newman, 1997; Ilan et al., 1999, 2000, 2001). Others have demonstrated that oxidant stressors such as hyperglycemia and hypoxia can affect PECAM-1 localization and phosphorylation (Kalra et al., 1996; Rattan et al., 1996, 1997; Pinter et al., 1999). Furthermore, VEGF-mediated dynamic tyrosine phosphorylation of PECAM-1 has been shown to modulate endothelial cell adhesion and migration (Esser et al., 1998). In development, PECAM-1 is expressed early in the presomite embryo in angioblasts and yolk sac blood islands and persists throughout embryonic cardiovascular development (Baldwin et al., 1994; Pinter et al., 1997). During initial stages of EMT in the heart, down-regulation of PECAM-1 occurs (Baldwin et al., 1994) followed by de-adhesion of individual mesenchymal cells from the endocardium. Matrix metalloproteinases (MMPs) such as MMP-2 are then expressed and play a role in cell migration and invasion (Alexander et al., 1997; Song et al., 2000).

In this paper, we demonstrate that high glucose has developmental stage-specific inhibitory effects on AV endocardial cushion EMT. In addition, our findings suggest that this hyperglycemic-induced disruption of EMT results from decreased VEGF-A expression, and is partially mediated by abnormal persistence of PECAM-1 and decreased MMP-2 expression.

Results

High glucose inhibits EMT of endocardial cells

We studied EMT in the developing heart using the endothelial cell marker PECAM-1 and the cushion mesenchymal cell marker α-smooth muscle actin (α-SMA, Fig. 1; DeRuiter et al., 1997; Nakajima et al., 1997). In a 9.5-days post coitus (dpc) murine heart, PECAM-1 is localized to the endocardium lining the AVC (boxed area) and outflow tract (boxed area; Fig. 1 A). Higher magnification (Fig. 1, B and C) illustrates EMT as seen by the presence of PECAM-1–positive endocardial cells lining the outflow tract (Fig. 1 B) and AVC (Fig. 1 C) and mesenchymal cells that have lost PECAM-1 expression and are migrating into the cardiac jelly. Fig. 1 (D and E) demonstrates the concomitant loss of endothelial and gain of mesenchymal markers in the invasive cells; the endocardial cells are PECAM-1–positive and α-SMA–negative, whereas endocardial cells undergoing EMT exhibit minimal to no PECAM-1 expression and are α-SMA–positive.

To assess the effects of high glucose at the onset of EMT (9.5 dpc), we used an in vitro model that recapitulates the cellular and molecular events of EC formation (Bernanke and Markwald, 1979, 1982; Runyan and Markwald, 1983). As illustrated in Fig. 2 (A and B), AV explants cultured in normal α-D-glucose exhibit robust EMT with cell separa-
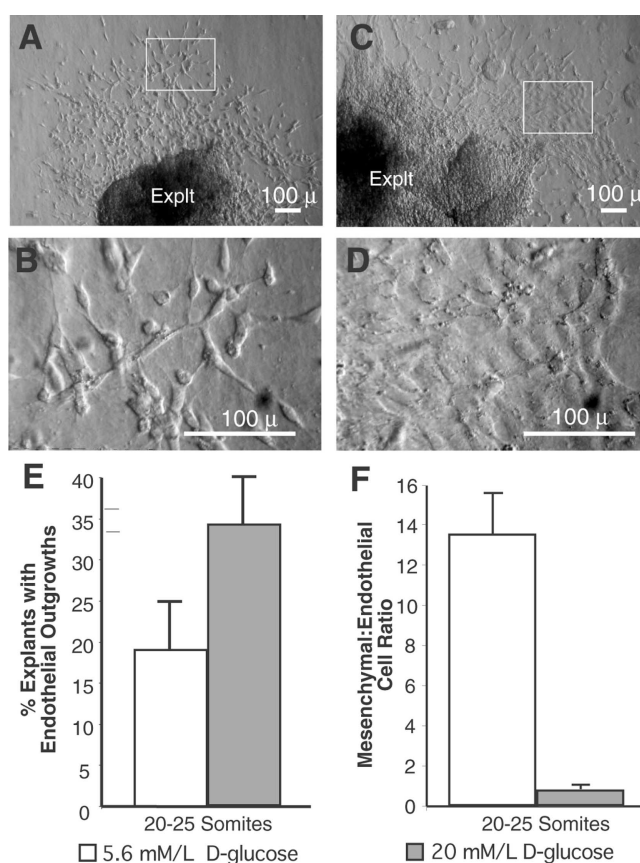

Figure 2. **Elevated α-D-glucose inhibits normal EC cell transformation in AVC explant cultures.** Light microscopic images of AVC explants from 9.5-dpc embryos are shown. Explants were cultured in normal (5.6 mM/L; A and B) and high (20 mM/L) α-D-glucose (C and D). A shows the outgrowth of transformed mesenchymal cells onto the collagen gel during EMT. B is a high power micrograph of the boxed area in A, illustrating the spindle-like morphology of migrating and invading mesenchymal cells. In contrast, C demonstrates the epithelioid-like sheet of nontransformed endocardial cells seen in elevated glucose conditions. D is a high power micrograph of the boxed area in C, illustrating the cobblestone-shaped cohesive endocardial cells. Bars, 100 μm. E shows the percentage + SEM of normal and high glucose-exposed AVC explants with an epithelioid-like phenotype, indicating lack of EMT specifically at the 20–25 somite stages. 5.6 mM/L D-glucose, $n = 84$; 20 mM/L D-glucose, $n = 97$; $P < 0.04$. (F) The extent of EMT in AVC explants cultured in normal versus high glucose conditions is represented as the ratio of mesenchymal to endothelial cells. This graph represents the mean + SEM of the cell counts from three independent litters. $n = 6$ for each condition, $P < 0.0001$.

tion, lateral migration of spindle-shaped cells, and cell invasion into the collagen gel (Fig. 3, A and B). In contrast, AV explants cultured in elevated α-D-glucose exhibit reduced EMT. Endocardial-derived cells migrate away from the explant as a confluent epithelioid sheet and fail to invade into the collagen gel (Fig. 2, C and D; Fig. 3, C and D).

The inhibitory effects of hyperglycemia on EMT are somite stage-specific

Somite number has been used as a staging method to determine temporal specificity of AVC EMT (Camenisch et al., 2002a). In our studies, the inhibitory effects of high glucose on EMT were significant ($P < 0.04$) at the 20–25 somite

Figure 3. **Endocardial cell PECAM-1 protein expression is retained and cell invasion is blocked in high glucose conditions.** Confocal fluorescence microscopic images of AVCs explanted at 9.5 dpc and cultured in normal (5.6 mM/L) and high (20 mM/L) α-D-glucose (C and D), then stained for PECAM-1 (red) and α-SMA (green). The top panel in A shows spindle-shaped α-SMA–positive cells dispersed on and invading (arrows, Z-plane; A, bottom) into the collagen gel (Z-plane; dashed lines demarcate the top of the collagen gel). B is a higher power micrograph illustrating the robust α-SMA and minimal PECAM-1 expression during EMT in normal glucose conditions. C shows α-SMA and PECAM-1–positive epithelioid-like cells that fail to invade into the collagen gel (Z-plane; dashed lines demarcate the top of the collagen gel). D is a higher power micrograph illustrating persistent PECAM-1 expression during failed EMT in high glucose conditions. Bars, 50 μm.
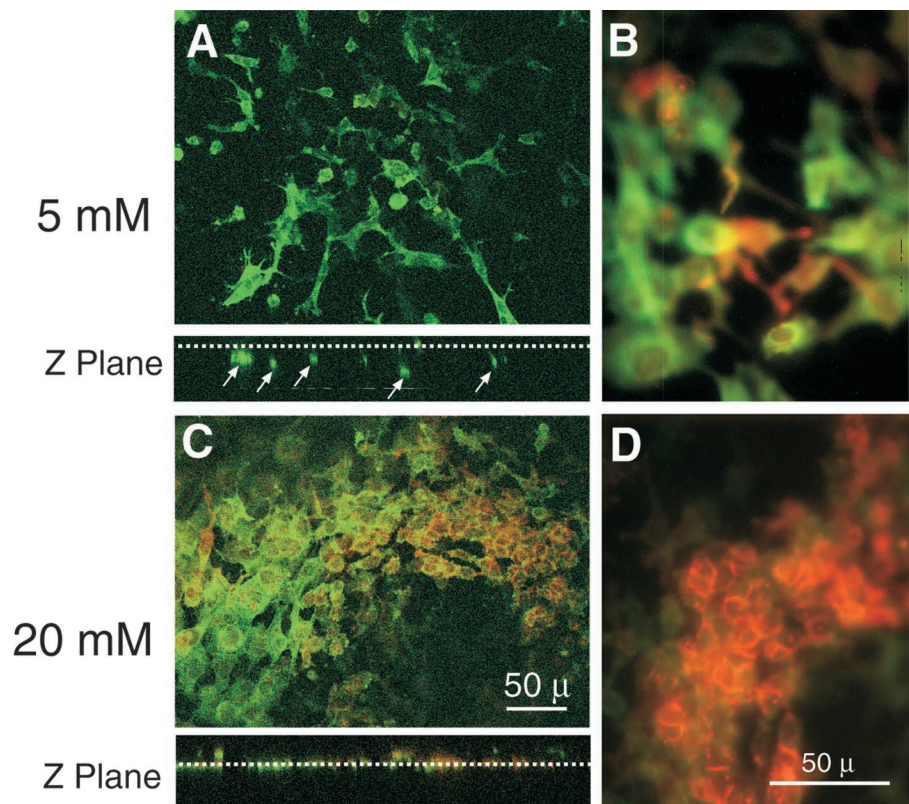
stage of development (Fig. 2 E), but not at earlier (<20 somites) or later (26–30 somites) developmental stages (unpublished data). Thus, disruption of EMT by a hyperglycemic insult occurs during a critical developmental window at the 20–25-somite stages, which is within the recently reported developmental time period for the onset of EMT in the mouse (Camenisch et al., 2002a). The effects of high glucose on EMT were further quantified by determining the ratio of mesenchymal to endothelial cell numbers as illustrated in Fig. 2 F. This inhibition of EMT by high glucose is illustrated as a marked drop in the mesenchymal to endothelial cell ratio (from 13.4 ± 5 to 0.75 ± 0.5; $P < 0.0001$).

Endocardial cells exhibit incomplete EMT in high glucose with persistence of PECAM-1 expression

To further assess EMT in normal and high glucose conditions, AVC explant cultures were immunolabeled using antibodies to PECAM-1 and α-SMA. In normoglycemic conditions, normal EMT occurs (Fig. 3, A and B) as seen by the presence of mesenchymal cells that migrate laterally away from the AVC explant and invade into the three-dimensional collagen gel (Z-plane; Fig. 3 A, bottom). These cells have lost PECAM-1 expression, express α-SMA, and exhibit cell separation typical of EMT. In high glucose conditions (Fig. 3, C and D), a confluent monolayer of cells is observed on the collagen gel surface (Z-plane; Fig. 3 C, bottom). These EC cells express α-SMA, and clusters of cells also maintain PECAM-1 expression (Fig. 3 D). Despite α-SMA expression, these cells are epithelioid in morphology, lack cell extensions characteristic of a migratory phenotype, and fail to invade the three-dimensional collagen gel. This suggests that down-regulation of endocardial PECAM-1 is a prerequisite step for normal EMT.

Hyperglycemic conditions elicit decreased myocardial VEGF expression in the AVC

To evaluate the level of VEGF-A expression associated with EC formation in murine conceptuses cultured in normal and high glucose conditions, we used transgenic mice containing a VEGF/LacZ bicistronic transcript (Miquerol et al., 1999; Pinter et al., 2001). Use of these mice allowed visualization of VEGF-A expression with the blue β-galactosidase reaction product LacZ (Fig. 4). In normal glucose conditions, VEGF-A was strongly expressed in the myocardium adjacent to the forming ECs. This correlated with robust EMT, as seen by the presence of mesenchymal cells throughout the underlying cardiac jelly (Fig. 4 A). In contrast, in high glucose conditions, the myocardium underlying the putative EC stains only faintly blue, indicating low VEGF-A expression. This correlated with a lack of EMT and complete absence of mesenchymal cells in the cardiac jelly (Fig. 4 B).

Exogenous recombinant mouse VEGF-A$_{165}$ abrogates and sequestration of endogenous VEGF mimics the effect of high glucose on AV cushion EMT

After the observation that high glucose elicits a reduction in myocardial VEGF expression in the area where EMT occurs, we hypothesized that the defect in AVC EMT could be rescued by supplementing high glucose cultures with recombinant mouse VEGF-A isoform 165 (rVEGF-A$_{165}$). As illustrated in Fig. 5 (A and C), AVC explants from 7.5-dpc conceptuses cultured in elevated α-D-glucose levels for 48 h exhibit an arrest of EMT, evidenced by outgrowths of confluent areas of cobblestone-like endocardial cells without appreciable migration into the gel (Fig. 5 C). Addition of 10 pg/ml of rVEGF-A$_{165}$ to the hyperglycemic
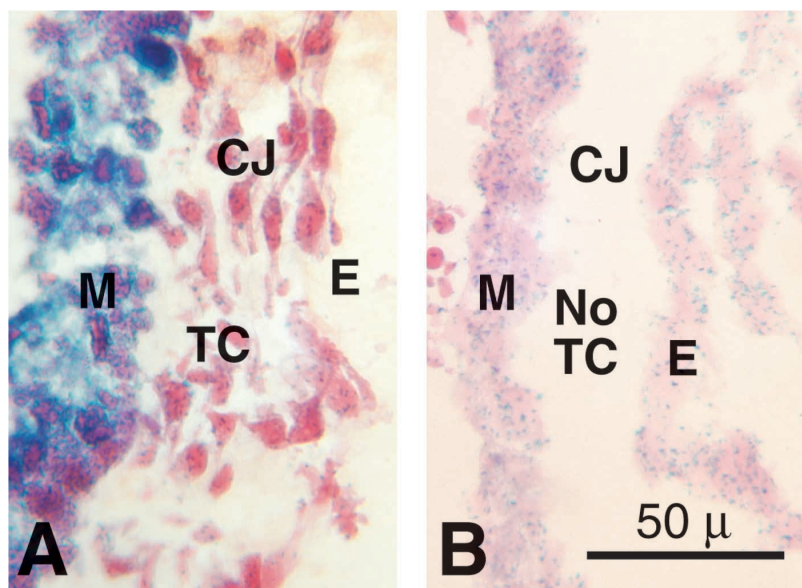
Figure 4.   **Myocardial VEGF-A expression is reduced in high glucose conditions and is required for EMT.** Light microscopic images demonstrating LacZ/VEGF staining in the AVC region from a 9.5-dpc embryo initially harvested at 7.5 dpc and placed in a whole conceptus culture for 48 h in either 5.6 mM/L (A) or 20 mM/L α-D-glucose (B). A is a representative section of an AVC cultured in 5.6 mM/L α-D-glucose. Note the intense blue staining of the myocardial layer (M) representing VEGF-A gene induction in contrast to the lack of myocardial staining in B. In A, note this area of EMT consisting of the endocardial layer (E) and transformed mesenchymal cells (TC) that have migrated into the underlying cardiac jelly (CJ). In contrast, B is a representative section of an AVC cultured in 20.0 mM/L α-D-glucose illustrating the AVC lined by endocardium (E) with complete lack of EMT; an acellular area of cardiac jelly (CJ) is present that lacks cushion mesenchyme (No TC). Bars, 50 μm.

conceptus cultures overcomes the glucose-induced arrest in EMT. Similar to control explants (Fig. 2 and Fig. 3), AVC explants from conceptus cultures supplemented with rVEGF-A_{165} exhibit restored EMT with multiple spindle-shaped mesenchymal cells dispersed onto the collagen gel surface (Fig. 5 B) and invading into the three-dimensional gel (Fig. 5 D).

To determine whether the effect of high glucose on cardiac cushion morphogenesis is mediated by decreased VEGF signaling, a soluble high-affinity VEGF receptor (sFlt-1) was added to 9.5-dpc AVC explant cultures to sequester bioavailable VEGF (Davis-Smyth et al., 1996; Gerber et al., 1999; Chow et al., 2001). sFlt-1 has previously been used to demonstrate that VEGF is a central mediator of hypoxia-induced defects in EC formation (Dor et al., 2001). As shown in Fig. 6 (D–F), explants treated with 25 μg/ml sFlt-1 retain an epithelioid phenotype and fail to invade into the collagen gel. As in high glucose conditions, endocardial cells are transitional, as evidenced by their α-SMA positivity. Thus, VEGF deficiency, whether primary or secondary to high glucose, produces a defect in EMT in the developing AV cushion.

MMP activity is required for mesenchymal cell invasion and MMP-2 is down-regulated in high glucose conditions

We examined the expression of MMP-2 in EC cells undergoing EMT in murine AVC explants cultured in the presence of normal and elevated glucose. Expression of MMP-2 (Fig. 7 B) is observed in the spindle-shaped α-SMA–positive mesenchymal cells (Fig. 7 A) invading the collagen gel. In contrast, the α-SMA–positive noninvading EC cells from high glucose-exposed explants exhibit a cohesive sheet-like morphology (Fig. 7 C) and are essentially devoid of MMP-2 expression (Fig. 7 D). Furthermore, 9.5-dpc AVC explant cultures treated with the MMP inhibitor GM6001 fail to exhibit invasion into three-dimensional collagen (Fig. 6, G–I). Induction of α-SMA was not affected in the presence of GM6001. This result suggests a specific role for MMPs in the invasion aspects of EMT.

PECAM-1 expression modulates EMT

Given the persistence of PECAM-1 expression in AVC endothelial cells exposed to elevated α-D-glucose (Fig. 3, C and D), we hypothesized that glucose-mediated changes in PECAM-1 signaling may play a role in disruption of EMT dur-
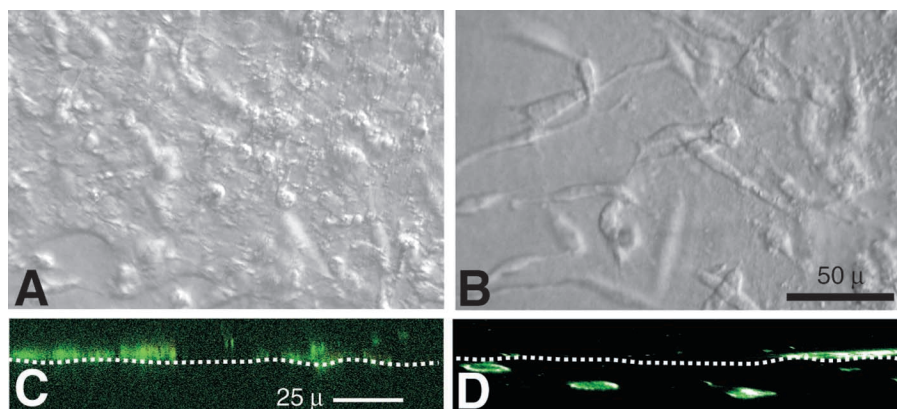

Figure 5.   **rVEGF-A_{165} rescues in vitro AVC morphogenesis in high glucose-treated embryos.** Light microscopic (A and B) and confocal immunofluorescence (C and D) images of 9.5-dpc AVC explants from whole conceptuses cultured in 20 mM/L α-D-glucose for 48 h starting from 7.5 dpc with (B and D) or without (A and C) 10 pg/ml rVEGF-A_{165}. A and C show an arrested EMT with extensive epithelioid endocardial cells on the surface of the gel devoid of any appreciable migration by the α-SMA–positive endocardial cells into the collagen gel (C). B and D illustrate the rescue of EMT in AVC explants from conceptuses cultured in high glucose and treated with 10 pg/ml of rVEGF-A_{165}. Note the outgrowth of spindle-shaped, transformed mesenchymal cells (B) and the migration of transformed α-SMA–positive cells into the gel. Bars: 50 μm for A and B; 25 μm for C and D.
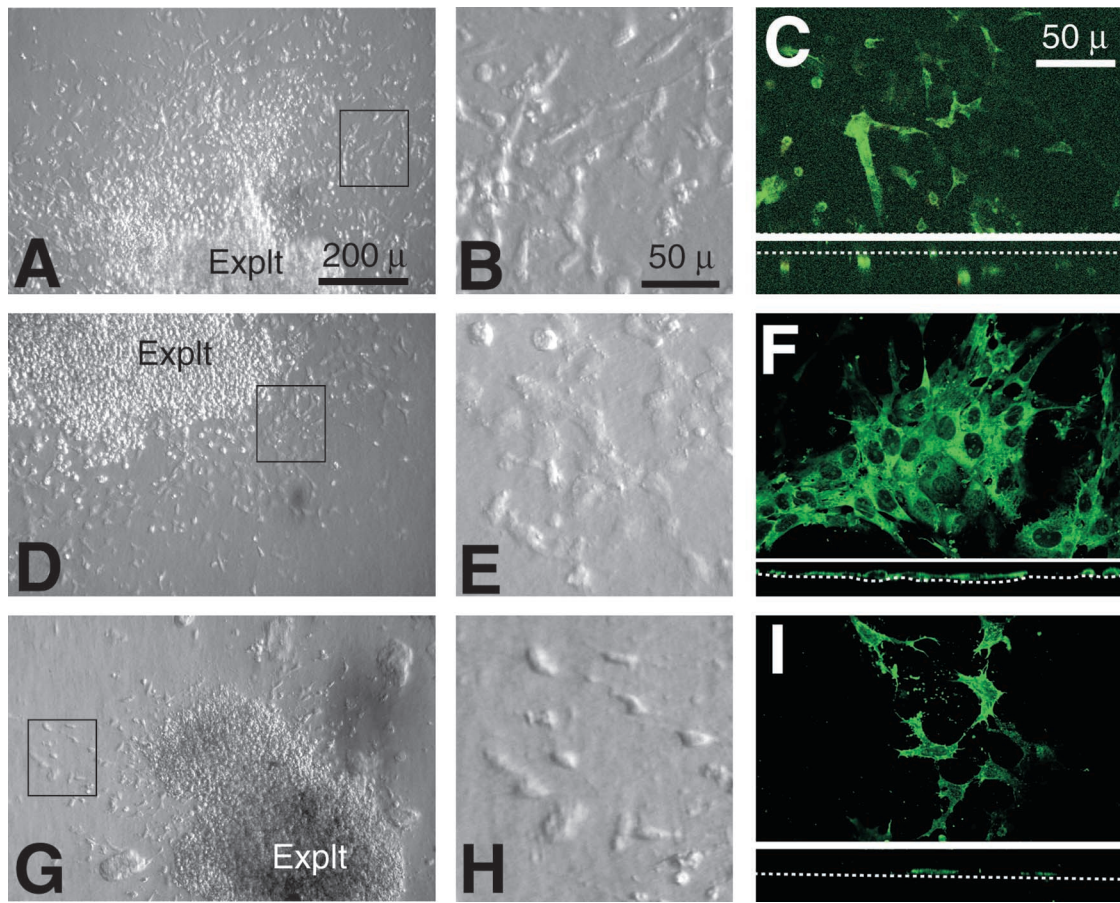
Figure 6. Sequestration of VEGF by sFlt-1 and inhibition of MMPs by GM6001 blocks EMT. Light and confocal fluorescence microscopic images of AVCs explanted at 9.5 dpc and cultured in 5.6 mM/L D-glucose alone (A–C), 5.6 mM/L D-glucose and 25 μg/ml sFlt (D–F), or 5.6 mM/L D-glucose and 10 μm GM6001 (G–I). B, E, and H are higher power micrographs of the areas boxed in A, D, and G. C, F, and I are representative en face (top) and Z-plane images (bottom) of endocardial cell outgrowths immunostained for α-SMA. Transformed mesenchymal cells exhibit cell–cell separation and invasion (A–C), in contrast to the sFLT-1–treated endocardial cells (D–F) that express α-SMA but are epithelioid in morphology, maintain their cell contacts, and fail to invade into the 3-D collagen gel (F, bottom). In G and H, GM6001-treated endocardial cells transform and migrate on the collagen gel; however, these α-SMA–positive mesenchymal cells fail to invade into the 3-D collagen gel (I, bottom). Dashed lines in C, F, and I represent the top of the collagen gels. Bars: 200 μm for A, D, and G; 50 μm for B, C, E, F, H, and I.

ing AVC morphogenesis. Therefore, we investigated the effects of elevated α-D-glucose on EC formation in PECAM-1–deficient mice. We find that explant cultures from PECAM-1–deficient mice exhibit normal EMT (compare Fig. 8 A with Fig. 2 B) even in the presence of elevated α-D-glucose levels (Fig. 8 B). In contrast to the high glucose-exposed wild-type explant cultures that exhibit inhibition of EMT (Fig. 2 C; Fig. 7, C and D), high glucose-exposed EC cells from PECAM-1–deficient mice undergo full transformation, including cell separation, invasion, and expression of MMP-2 (Fig. 8, C and D). Thus, retention of PECAM-1 expression appears to mediate the abnormal cohesive phenotype seen in high glucose-exposed EC cells.

PECAM-1 modulates endothelial cell morphology, individual cell motility, and MMP-2 expression in cell culture

The failure of high glucose to inhibit spindle-shaped cell morphology, cell separation and motility, and MMP-2 expression in PECAM-1–deficient EC cells led us to evaluate these parameters in cultured immortalized PECAM-1–defi-cient endothelial cells. As illustrated in Fig. 9 A, the PECAM-1/CD31-knock-out (KO) cells display a spindle-shaped morphology similar to that of cushion mesenchymal cells (Fig. 9 A, upper left panel), whereas the CD31-RC (PECAM-1 reconstituted, or RC) cells display a rounded, epithelioid morphology similar to that seen with EMT inhibition (Fig. 9 A, lower left panel). When sparsely plated cells were stained for F-actin, the differences in morphology are more apparent, highlighting the spindle shape and extension formation of CD31-KO cells (Fig. 9 A, upper right panel) as compared with the rounded CD31-RC cells (Fig. 9 A, lower right panel).

In addition to a change in cell morphology, EC cells that have undergone EMT normally display extensive single cell motility away from the explant on the type I collagen gel in contrast to the sheet-like migration observed in glucose-induced inhibition of EMT. To further assess the role of PECAM-1 in cell motility, studies were performed using CD31-KO and CD31-RC endothelial cells to assess nondirected single cell motility through 8-μm pores in type I collagen–coated transwell membranes. As illustrated in Fig. 9
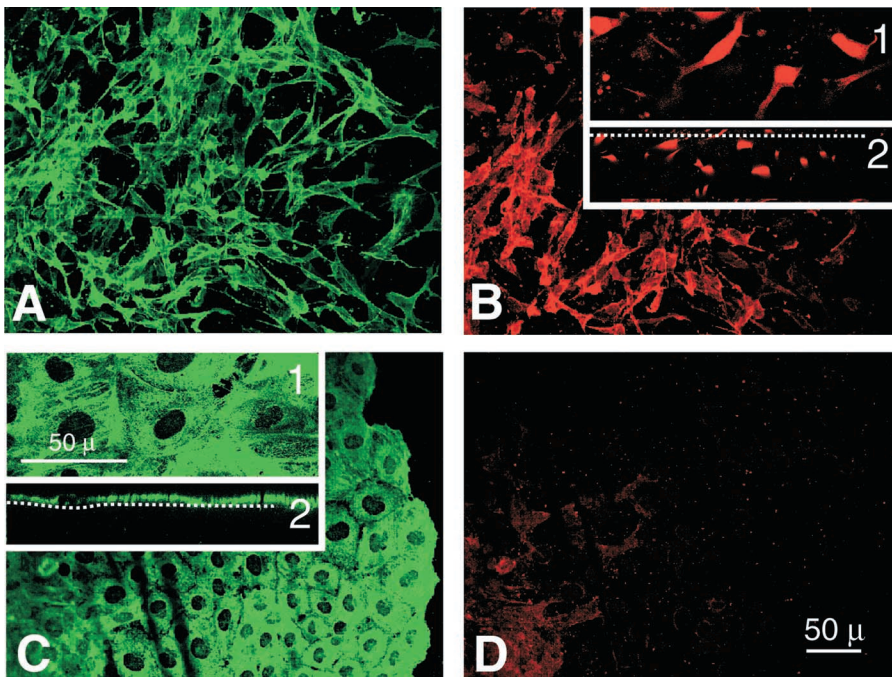
Figure 7. **MMP-2 expression is down-regulated in high glucose conditions and is required for invasion.** Confocal images of endocardial cell outgrowths from 9.5-dpc AVC explants cultured in 5.6 mM/L (A and B) or 20 mM/L α-D-glucose (C and D) and immunostained for α-SMA (A and C, green) and MMP-2 (B and D, red). A and B are representative of the spindle-shaped, transformed mesenchymal cells that exhibit α-SMA (A) and MMP-2 (B) expression. 1 B is a higher power image of transformed cells with MMP-2 staining. 2 B is a Z-plane illustrating invading transformed cells. C and D demonstrate cohesive, epithelioid-like, incompletely transformed EC cells expressing α-SMA (C) but minimal MMP-2 (D). 1 C Is a higher power en face image of α-SMA–positive endocardial cells, and 2 C is a Z-plane illustrating restriction of these cells to the collagen gel surface. Bars, 50 μm. Dashed lines in 2 B and 2 C represent the top of the collagen gels.

B, the CD31-KO endothelial cells transmigrate at a rate that is fivefold greater than the CD31-RC cells. Similar to our observations in the AVC explant cultures, PECAM-1-KO endothelial cells were resistant to high glucose-mediated inhibition of single cell motility (unpublished data).

Given the inverse correlation between PECAM-1 and MMP-2 expression in EC cells undergoing EMT (compare Fig. 3 and Fig. 7) and the importance of MMP activity for mesenchymal cell invasion (Fig. 6 and Fig. 7), we assessed the expression of MMP-2 in CD31-KO and CD31-RC endothelial cells. As seen in the representative Western blot in Fig. 9 C, CD31-KO cells express significantly more MMP-2 than do CD31-RC cells. Increased MMP-2 activity in CD31-KO cells compared with CD31-RC cells was confirmed by gelatin zymography (Fig. 9 D). Thus, our findings suggest that loss of PECAM-1 expression promotes acquisition of a mesenchymal cell phenotype with spindle-shaped morphology, enhanced single cell motility, and the robust induction of MMP-2 required for cell invasion.

Discussion

We have investigated the effects of hyperglycemia on AVC EMT. The use of whole conceptus and AVC explant assays have allowed us to investigate the teratogenic effects of elevated α-D-glucose on the forming ECs, which represent a small, defined area in the embryonic heart with two specific tissue layers (endocardium and myocardium) and a limited subpopulation of cells. These systems permit evaluation of the effects of a single factor at a specific stage of embryonic development while maintaining normal anatomic relationships between tissue layers, and allowing for physiologically relevant signaling between these different layers. Our results reveal that the teratogenic effects of glucose on EMT are developmental stage specific. An insult in mice had no effect unless timed at the 20–25-somite stages, which corresponds to the developmental window coincident with the onset of EMT (Fig. 2 E; Camenisch et al., 2002a). High glucose at this stage resulted in partial transformation of EC cells and
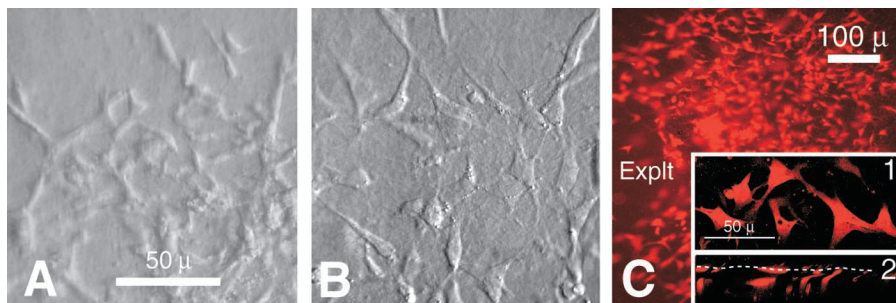

Figure 8. **PECAM-1–deficient mice undergo normal EMT in high glucose conditions.** Light and confocal fluorescence microscopic images of AVC explants from 9.5-dpc embryos from PECAM-1–deficient (CD31 KO) mice cultured in 5.6 mM/L (A) or 20 mM/L α-D-glucose (B and C). A illustrates CD31 KO–derived AVC explants in 5.6 mM/L α-D-glucose exhibiting normal EMT, evidenced by the outgrowth of spindle-shaped, transformed endocardial cells. B illustrates normal EMT in CD31 KO–derived AVC explants in the presence of 20 mM/L α-D-glucose. C is a representative en face confocal fluorescence image of a CD31 KO–derived AVC explant cultured in 20 mM/L α-D-glucose exhibiting normal EMT, evidenced by the outgrowth of MMP-2–positive spindle-shaped, transformed endocardial cells. The insets are higher power en face (1 C) and Z-plane (2 C) confocal sections illustrating robust MMP-2–positive cells that are migrating into the collagen gel (dashed line in 2 D denoted the surface of the gel). Bars: 100 μm for A and B; 50 μm for C; and 50 μm for 1 C and 2 C.

Figure 9. **PECAM-1 modulates endothelial cell morphology, single cell motility, and MMP-2 expression.** (A) Representative light (left panels) and actin fluorescence microscopic images (right panels) illustrating distinct morphologies of CD31-KO and CD31-RC cells plated on type I collagen. Note the spindle shape and extension formation of the CD31-KO cells (A, top panels) in contrast to the epithelioid appearance of the CD31-RC cells (A, bottom panels). Bars: 50 μm for left panels; 25 μm for right panels. (B) CD31-KO and RC cell transmigration through type I collagen–coated 8-μm pore transwells. Illustrated is a fivefold increase in nondirected single cell motility of CD31-KO vs. RC cells over 4 h ($n = 8$; $P < 0.00001$). Although the transmigration rate of CD31-KO cells was not affected by the addition of 20 mM/L of α-D-glucose, the CD31-RC cells exhibited a 34% decrease in motility in the presence of 20 mM/L α-D-glucose (not depicted). (C) Representative Western blot and (D) gelatin zymography illustrating increased MMP-2 expression (C) and activity (D) in the CD31-KO lysate compared with the CD31-RC lysate.
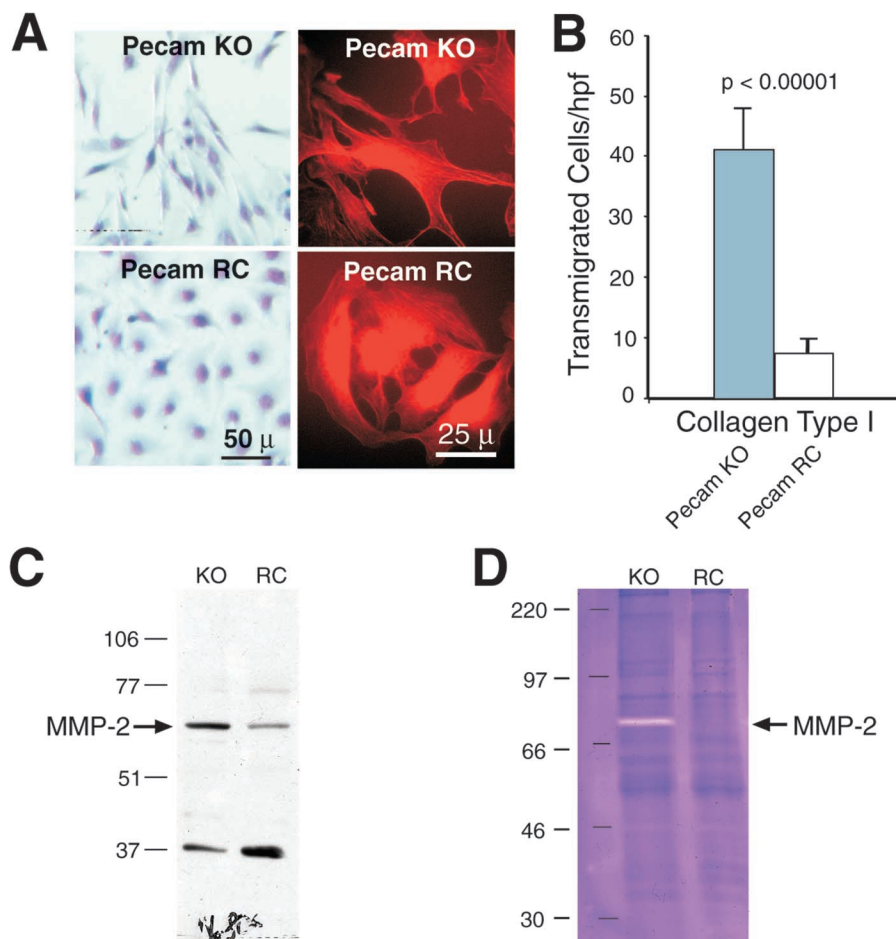
inhibited cell separation and single cell migration and invasion (Fig. 2, C and D; Fig. 3 C).

Consistent with previous studies demonstrating the necessity of maintaining appropriate levels of VEGF-A for proper yolk sac vasculogenesis and cardiac morphogenesis (Miquerol et al., 2000; Dor et al., 2001; Pinter et al., 2001; Damert et al., 2002), we find that glucose-induced reduction in myocardial VEGF-A expression in the AVC results in inhibition of EMT. The effect of glucose on VEGF-A expression mirrors our previous findings in the yolk sac, where high glucose-induced reduction of endodermal VEGF-A was correlated with an arrest in yolk sac vasculogenesis at the primary plexus stage (Pinter et al., 2001). In both studies, exogenous rVEGF-A$_{165}$ in a tight concentration range rescued yolk sac vasculogenesis (2–10 pg/ml) and EC cell outgrowth (10 pg/ml; Fig. 5, C and D). Furthermore, sequestration of endogenous VEGF with the recombinant receptor sFlt-1 at the onset of EMT was sufficient to block EMT at this stage of cushion development under normal glucose conditions (Fig. 6, D–F). Other investigators have demonstrated that decreased VEGF-A levels result in embryonic lethality at 9 dpc, secondary to abnormal yolk sac blood island formation and vascularization (Ferrara et al., 1996; Damert et al., 2002). There is evidence to suggest that VEGF-mediated dynamic tyrosine phosphorylation of cell junction proteins such as VE-cadherin and PECAM-1 may be an important modulatory step of endothelial cell adhesion and migration (Esser et

al., 1998). Our results demonstrate that hyperglycemia-induced reductions in VEGF-A expression during early precardiac mesodermal differentiation, and later during EC formation, can result in endocardial cell migration defects. These findings suggest that reduced VEGF-A levels may also result in transient changes in tyrosine phosphorylation of cell adhesion molecules such as PECAM-1, leading to persistent adhesion between endothelial cells, preventing disassociation of these cells from the endocardium, and consequently reducing the number of migrating EC cells. In addition, reduction in VEGF-A signaling may result in incomplete transformation of endocardial cells that have de-adhered from the endocardium, thereby affecting their ability to migrate as single cells and invade into the ECM.

In this paper, we show that PECAM-1 and MMP-2 have a modulatory role in the process of EMT (Fig. 10). The endocardium is an epithelium composed of endothelial cells, and as seen in Fig. 1 D, transformed endocardial cells lose expression of endothelial PECAM-1 coincident with the gain of expression of the mesenchymal marker α-SMA. High glucose-treated AVC explants (Fig. 2, C and D; Fig. 3, C and D) exhibit a transitional phenotype expressing α-SMA and retaining PECAM-1 expression. Unlike the invasive mesenchymal cells in untreated explants, these transitional epithelioid cells fail to express MMP-2 (Fig. 7 D). Furthermore, the MMP inhibitor GM6001 specifically blocks cell invasion (Fig. 6 F, bottom), underscoring the functional significance of lack of MMP-2 expression in
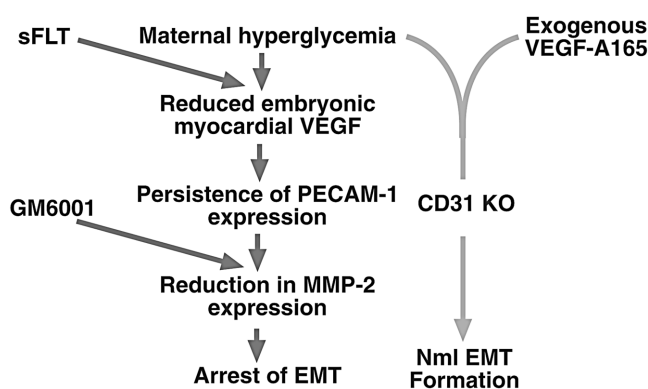
Figure 10. **Flow chart depicting the putative cascade of effects initiated by high glucose on AVC morphogenesis.** Inhibitory effects of hyperglycemia on EMT can be mimicked by sequestration of VEGF by addition of sFlt or by addition of GM6001. These effects are abrogated by exogenous rVEGF-A$_{165}$ (in a specific dose range) or by eliminating endocardial PECAM-1 expression through the use of the PECAM-1–deficient mouse (CD31 KO).

PECAM-1–positive, noninvading high glucose-treated endocardial cells (Fig. 7 D).

As seen in Fig. 8, AVC explants from PECAM-1–deficient mice cultured in high glucose undergo complete EMT with dispersal of MMP-2–expressing mesenchymal cells that invade the ECM. This result indicates that loss of PECAM-1 is sufficient to rescue complete EMT in the presence of high glucose. Furthermore, immortalized endothelial cells derived from PECAM-1–deficient mice (CD31-KO) morphologically resemble transformed endocardial cells with their spindle-like shape and extension formation (Fig. 9 A). Compared with cells reconstituted with physiologic levels of full-length murine PECAM-1 (CD31-RC) and reminiscent of their mesenchymal counterparts, CD31-KO cells have significantly increased nondirected single cell motility and are resistant to glucose inhibition (Fig. 9 B) in transwell transmigrations through type I collagen–coated membranes. Furthermore, CD31-KO endothelial cells have higher expression levels and activity of MMP-2 than do CD31-RC endothelial cells (Fig. 9, C and D). These observations suggest that PECAM-1 may function in a similar fashion to members of the cadherin family, whose engagement causes down-regulation of MMP expression and activity. Conversely, loss of cadherin expression (specifically, E-cadherin) has been shown to elicit increases in MMP expression and invasiveness in several cell systems (Anzai et al., 1996; Llorens et al., 1998).

This work provides supportive evidence that diabetic embryopathy is a phenomenon of poor glycemic control during early gestation that can perturb normal cardiovascular development. We have shown that the teratogenic effects of elevated α-D-glucose on the developing AV ECs involve VEGF-A–mediated defects in endocardial cell transformation, migration, and invasion. Future studies are needed to understand how VEGF-A modulates PECAM-1 expression and phosphorylation state in EC cells, how PECAM-1 in turn regulates MMP expression, and how loss of PECAM-1 overrides the inhibitory effect of hyperglycemia on EMT. Defects of the AV valves and septa are the most commonly

observed congenital heart malformations, and further dissection of the complex molecular mechanisms of AVC morphogenesis from both normal and pathological standpoints can lead to insights into preventing congenital cardiac anomalies.

Materials and methods

Mice
Conceptuses were harvested from timed pregnant CD1 (Charles River Laboratories), C57/BL6J (Jackson ImmunoResearch Laboratories), PECAM-1–deficient (Mahooti et al., 2000; Graesser et al., 2002), and VEGF-LacZ-knock-in CD1 heterozygous mice (Miquerol et al., 1999; Pinter et al., 2001). All procedures were performed in accordance with established, approved Yale University Animal Care Committee protocols.

Antibodies
Antibodies for immunocytochemistry and Western blotting are as follows: mouse monoclonal anti-α-SMA (Sigma-Aldrich); rabbit polyclonal anti-PECAM-1 (Pinter et al., 1997, 1999); rabbit polyclonal anti-MMP-2 Ab809 (CHEMICON International); Alexa Fluor® 488 goat anti–mouse IgG and Alexa Fluor® 595 goat anti–rabbit IgG (Molecular Probes, Inc.); rhodamine-phalloidin (Sigma-Aldrich); secondary donkey anti–rabbit HRP-conjugated Ab (Amersham Biosciences), affinity-purified polyclonal anti–vimentin (Haas et al., 1998).

AVC EC explant assay
As described in Camenisch et al. (2000 and 2002a), AVC explants (atrioventricular canal and ventricle) were dissected out from 9.5-dpc embryos and placed on rat tail-type I collagen gels (BD Biosciences), and were prehydrated for a minimum of 1 h with 100 ml of Medium 199 supplemented with 1% FBS, 100 U/ml penicillin, 100 μg/ml streptomycin, and 0.1% each of insulin, transferrin, and selenium (GIBCO BRL). AV explants were incubated at 37°C in 5% CO$_2$. 100 μl of Medium 199 was added. Embryos treated with either α-D-glucose (Sigma-Aldrich) at 20 mM/L, 25 μg/ml of the soluble murine recombinant VEGF receptor 1/IgG-Fc chimeric protein sFlt-1 (mFlt(1–3)-IgG, a truncated Flt 1–3 Fc fusion protein; a gift from Dr. N. Ferrara, Genentech, San Francisco, CA; van Bruggen et al., 1999), or 10 μM of the MMP inhibitor GM6001 (Ilomastat; AMS Scientific Inc.) were exposed to the indicated reagent for 30 min before AVC explantation and were then cultured in Medium 199 containing the specific reagent. At 48 h, cultures were stopped and the ventricular myocardium was removed.

Quantification of EMT was accomplished using two morphologically based methods. In the first method, AVC explants from 9.5-dpc embryos were cultured in normal and high glucose conditions and assessed for the presence of a confluent epithelioid sheet. 9.5-dpc embryos varied in somite number, and therefore, were divided into groups according to somite number (<20, 20–25, and 26–30 somites). Normal and high glucose-exposed explants from somite stages 20–25 versus somite stages 26–30 exhibited areas of confluent epithelioid-like cells (Pinter et al., 2001). The percentage of AVC explants exhibiting a confluent epithelioid in both normal and high glucose conditions was determined and compared using a Z-test analysis. In the second method, using the quantification methods previously described by Camenisch et al. (2002b), the extent of EMT was assessed by determining the ratio of number of mesenchymal versus epithelioid-like cells in a subset of normal and high glucose-exposed explants randomly selected from three separate independent experiments. Statistics were performed using a one-way ANOVA.

Whole conceptus culture
7.5-dpc murine conceptuses were harvested from timed pregnant WT CD1 female mice mated with male VEGF-LacZ-heterozygous mice and cultured as described previously (Pinter et al., 1999, 2001). 20 mM/L α-D-glucose with or without 10 pg/ml recombinant mouse VEGF-A$_{165}$ (CHEMICON International) was added to normoglycemic cultures.

Staining of embryos
β-Galactosidase staining: After a 48-h culture period in normal and hyperglycemic conditions, embryos were fixed in 2% PFA and 0.2% glutaraldehyde at RT for 30 min and washed three times in PBS. Staining was performed overnight at 37°C in 0.02% glutaraldehyde, 5 mM K$_3$Fe(CN)$_6$, 5 mM K$_4$Fe(CN)$_6$, and 2 mM MgCl$_2$ in PBS as described previously (Miquerol et al., 1999; Pinter et al., 2001). Embryos were rinsed three times with PBS, embedded in M-1 embedding matrix (Shandon, Inc.), snap frozen in isopentane cooled in liquid nitrogen, and sectioned at 5

μm onto UltraStick® glass slides (Fisher Scientific). Sections were counter-stained red with 0.13% safranin.

Immunoperoxidase staining: Embryos were fixed in 4% PFA, snap frozen in isopentane cooled in liquid nitrogen, sectioned, and mounted on glass slides as described previously (Pinter et al., 1997). Immunostaining was performed using the avidin–biotin complex technique (ABC kit; Vector Laboratories). Sections were incubated with anti-PECAM-1 followed by incubation with secondary biotinylated goat anti–rabbit antibody. After incubation in avidin-peroxidase, staining was visualized using a DAB reaction as described previously (Pinter et al., 1997).

Fluorescence and confocal microscopy

AV EC cells embedded in the collagen gel were fixed with 4% PFA, rinsed with PBS, permeabilized with 0.5% Triton X-100, 10 mM Pipes, pH 6.8, 50 mM NaCl, 300 mM sucrose, and 3 mM $MgCl_2$, and blocked overnight at 4°C in 3% BSA and 0.5% Tween 20 in PBS. For double immunostaining, cells were incubated with a 1:400 dilution of anti-αSMA Ab and a 1:250 dilution of anti-PECAM-1 Ab or a 1:200 dilution of anti-MMP-2 Ab overnight at 4°C, washed with 0.2% BSA and 0.5% Tween 20 in PBS, then incubated in a 1:200 dilution of Alexa Fluor® 488 goat anti–mouse IgG and Alexa Fluor® 595 goat anti–rabbit IgG. Fluorescence microscopy images were obtained with a Research Fluorescence Microscope (Carl Zeiss MicroImaging, Inc.) equipped with a SPOT™ camera. Images were collected and stored using Adobe Photoshop® 5.0 on an Apple Macintosh G3 computer.

Confocal images were obtained using an inverted microscope (IX70; Olympus) equipped with an Argon/Krypton scanning laser system (FluoView™; Olympus). En face and Z-plane sections were obtained using FluoView™ software (Olympus).

Cell culture

PECAM-KO (CD31-KO) endothelioma cell line luEND.PECAM-1.1 was established by retroviral transduction of primary endothelial cell culture with the polyoma virus middle T-oncogene. CD31-KO cells were then retrovirally transduced with full-length murine PECAM-1 cDNA as described previously, generating a PECAM-1 RC (CD31-RC) cell line (Wong et al., 2000; Graesser et al., 2002). The endothelioma cell lines retained surface expression of VE-cadherin by FACS® and showed contact inhibition on confluence. Cells were cultured in DME with 10% FBS, 10 mM Hepes, pH 7.4, 1% L-glutamine, 1% nonessential amino acids, 1% pyruvate, 10,000 U/ml penicillin/streptomycin, and 10^5 M 2-mercaptoethanol (GIBCO BRL) and were incubated at 37°C in 8% CO_2. Selection of PECAM-1 expression on CD31-RC cells was maintained with 1 μg/ml puromycin.

Motility assay

8.0-μm pore size 6.5-mm diam transwell (Corning Incorporated) were coated overnight with 12.5 μg/ml type I collagen and blocked with 5% BSA as described previously (Haas et al., 1998). 100 μl of media was added to the top well and 500 μl to the bottom well. Endothelial cells were trypsinized, washed twice in endothelial media, and 100 μl of a 10^6-cells/ml single cell suspension was added to the top well. After 2.5 h of incubation at 37°C in 8% CO_2, the cells were washed once with TBS, fixed in Streck's Tissue Fixative (STF; Streck Laboratories), and stained with crystal violet. Cells on the top surface of the filter were removed with a cotton swab and cells on the bottom surface were quantitated.

For immunofluorescence staining, cells were incubated overnight on 8-chamber glass culture slides (Falcon; BD Biosciences) coated with type I collagen as above. Cells were washed once with TBS, fixed in STF, permeabilized with 0.5% Triton X-100 in TBS, and stained with rhodamine-phalloidin.

Western blotting and zymography

Cells were lysed in 120 mM Tris-HCl buffer, pH 8.7, 0.1% Triton X-100, 0.01% sodium azide, and 5% glycerol. For Western blotting, 25 μg protein was electrophoresed on an 8% SDS-PAGE gel and then blotted onto a PVDF membrane. Membranes were blocked for 30 min in TBS containing 0.05% Tween 20 and 5% milk, hybridized overnight at 4°C with anti-MMP-2 Ab, then incubated with a secondary donkey anti–rabbit HRP-conjugated Ab and chemiluminescent detection (SuperSignal®; Pierce Chemical Co.). Blots were normalized by stripping and reblotting with anti–vimentin Ab to ensure equal loading of all samples. For zymography, 20 μg protein per sample was prepared in nondenaturing loading buffer and size fractionated in a 10% SDS-polyacrylamide gel impregnated with 0.4% gelatin (Haas et al., 1998). The gels were washed in 2.5% Triton X-100, washed two times with water, then incubated for 24 h at 37°C in a 50-mM Tris-HCl buffer, pH 8.0, containing either 5 mM calcium chloride or 10 mM EDTA (negative control for MMP activity). Gels were fixed in 50% methanol and 10% acetic acid containing 0.1% Coomassie Blue

R250, dried, and then scanned (300 d.p.i.) using an Arcus II scanner (AgFa-Gevaert N.V.).

References

Alexander, S.M., K.J. Jackson, K.M. Bushnell, and P.G. McGuire. 1997. Spatial and temporal expression of the 72-kDa type IV collagenase (MMP-2) correlates with development and differentiation of valves in the embryonic avian heart. *Dev. Dyn.* 209:261–268.

Anzai, H., Y. Kitadai, C.D. Bucana, R. Sanchez, R. Omoto, and I.J. Fidler. 1996. Intratumoral heterogeneity and inverse correlation between expression of E-cadherin and collagenase type IV in human gastric carcinomas. *Differentiation.* 60:119–127.

Baldwin, H.S., H.M. Shen, H.C. Yan, H.M. DeLisser, A. Chung, C. Mickanin, T. Trask, N.E. Kirschbaum, P.J. Newman, S.M. Albelda, et al. 1994. Platelet endothelial cell adhesion molecule-1 (PECAM-1/CD31): alternatively spliced, functionally distinct isoforms expressed during mammalian cardiovascular development. *Development.* 120:2539–2553.

Bernanke, D.H., and R.R. Markwald. 1979. Effects of hyaluronic acid on cardiac cushion tissue cells in collagen matrix cultures. *Tex. Rep. Biol. Med.* 39:271–285.

Bernanke, D.H., and R.R. Markwald. 1982. Migratory behavior of cardiac cushion tissue cells in a collagen-lattice culture system. *Dev. Biol.* 91:235–245.

Boughman, J.A., C.A. Neill, C. Ferencz, and C.A. Loffredo. 1993. The genetics of congenital heart disease. *In* Epidemeology of Congenital Heart Disease: The Baltimore-Washington Infant Study, 1981–1989. C. Ferencz, J.D. Rubin, C.A. Loffredo, and C.A. Magee, editors. Futura Publishing Co., Mount Kisco, NY. 123–167.

Boyer, A.S., and R.B. Runyan. 2001. TGFbeta Type III and TGFbeta Type II receptors have distinct activities during epithelial-mesenchymal cell transformation in the embryonic heart. *Dev. Dyn.* 221:454–459.

Boyer, A.S., I.I. Ayerinskas, E.B. Vincent, L.A. McKinney, D.L. Weeks, and R.B. Runyan. 1999a. TGFbeta2 and TGFbeta3 have separate and sequential activities during epithelial-mesenchymal cell transformation in the embryonic heart. *Dev Biol.* 208:530–545.

Boyer, A.S., C.P. Erickson, and R.B. Runyan. 1999b. Epithelial-mesenchymal transformation in the embryonic heart is mediated through distinct pertussis toxin-sensitive and TGFbeta signal transduction mechanisms. *Dev. Dyn.* 214:81–91.

Camenisch, T.D., A.P. Spicer, T. Brehm-Gibson, J. Biesterfeldt, M.L. Augustine, A. Calabro, Jr., S. Kubalak, S.E. Klewer, and J.A. McDonald. 2000. Disruption of hyaluronan synthase-2 abrogates normal cardiac morphogenesis and hyaluronan-mediated transformation of epithelium to mesenchyme. *J. Clin. Invest.* 106:349–360.

Camenisch, T.D., D.G.M. Molin, A. Person, R.B. Runyan, A.C. Gittenberger-de Groot, J.A. McDonald, and S.E. Klewer. 2002a. Temporal and distinct TGFβ ligand requirements during mouse and avian endocardial cushion morphogenesis. *Dev. Biol.* 248:170–181.

Camenisch, T.D., J.A. Schroeder, J. Bradley, S.E. Klewer, and J.A. McDonald. 2002b. Heart-valve mesenchyme formation is dependent on hyaluronan-augmented activation of ErbB2 ErbB3 receptors. *Nat. Med.* 8:850–855.

Carmeliet, P., V. Ferreira, G. Breier, S. Pollefeyt, L. Kieckens, M. Gertsenstein, M. Fahrig, A. Vandenhoeck, K. Harpal, C. Eberhardt, et al. 1996. Abnormal blood vessel development and lethality in embryos lacking a single VEGF allele. *Nature.* 380:435–439.

Chow, J., O. Ogunshola, S.Y. Fan, Y. Li, L.R. Ment, and J.A. Madri. 2001. Astrocyte-derived VEGF mediates survival and tube stabilization of hypoxic brain microvascular endothelial cells in vitro. *Brain Res. Dev. Brain Res.* 130:123–132.

Damert, A., L. Miquerol, M. Gertsenstein, W. Risau, and A. Nagy. 2002. Insuffi-

cient VEGFA activity in yolk sac endoderm compromises haematopoietic and endothelial differentiation. *Development.* 129:1881–1892.

Davis-Smyth, T., H. Chen, J. Park, L.G. Presta, and N. Ferrara. 1996. The second immunoglobulin-like domain of the VEGF tyrosine kinase receptor Flt-1 determines ligand binding and may initiate a signal transduction cascade. *EMBO J.* 15:4919–4927.

DeLisser, H.M., M. Christofidou-Solomidou, R.M. Strieter, M.D. Burdick, C.S. Robinson, R.S. Wexler, J.S. Kerr, C. Garlanda, J.R. Merwin, J.A. Madri, and S.M. Albelda. 1997. Involvement of endothelial PECAM-1/CD31 in angiogenesis. *Am. J. Pathol.* 151:671–677.

DeRuiter, M.C., R.E. Poelmann, J.C. VanMunsteren, V. Mironov, R.R. Markwald, and A.C. Gittenberger-de Groot. 1997. Embryonic endothelial cells transdifferentiate into mesenchymal cells expressing smooth muscle actins in vivo and in vitro. *Circ. Res.* 80:444–451.

Dor, Y., T.D. Camenisch, A. Itin, G.I. Fishman, J.A. McDonald, P. Carmeliet, and E. Keshet. 2001. A novel role for VEGF in endocardial cushion formation and its potential contribution to congenital heart defects. *Development.* 128:1531–1538.

Erickson, S.L., K.S. O'Shea, N. Ghaboosi, L. Loverro, G. Frantz, M. Bauer, L.H. Lu, and M.W. Moore. 1997. ErbB3 is required for normal cerebellar and cardiac development: a comparison with ErbB2-and heregulin-deficient mice. *Development.* 124:4999–5011.

Esser, S., M.G. Lampugnani, M. Corada, E. Dejana, and W. Risau. 1998. Vascular endothelial growth factor induces VE-cadherin tyrosine phosphorylation in endothelial cells. *J. Cell Sci.* 111:1853–1865.

Ferrara, N., K. Carver-Moore, H. Chen, M. Dowd, L. Lu, K.S. O'Shea, L. Powell-Braxton, K.J. Hillan, and M.W. Moore. 1996. Heterozygous embryonic lethality induced by targeted inactivation of the VEGF gene. *Nature.* 380:439–442.

Gerber, H., T.H. Vu, A.M. Ryan, J. Kowalski, Z. Werb, and N. Ferrara. 1999. VEGF couples hypertrophic cartilage remodeling, ossification and angiogenesis during endochondral bone formation. *Nat. Med.* 5:623–628.

Graesser, D., A. Solowiej, M. Bruckner, E. Osterweil, A. Juedes, S. Davis, N.H. Ruddle, B. Engelhardt, and J.A. Madri. 2002. Altered vascular permeability and early onset of experimental autoimmune encephalomyelitis in PECAM-1-deficient mice. *J. Clin. Invest.* 109:383–392.

Haas, T.L., S.J. Davis, and J.A. Madri. 1998. Three-dimensional type I collagen lattices induce coordinate expression of matrix metalloproteinases MT1-MMP and MMP-2 in microvascular endothelial cells. *J. Biol. Chem.* 273:3604–3610.

Ilan, N., S. Mahooti, D.L. Rimm, and J.A. Madri. 1999. PECAM-1 (CD31) functions as a reservoir for and a modulator of tyrosine-phosphorylated beta-catenin. *J. Cell Sci.* 112:3005–3014.

Ilan, N., L. Cheung, E. Pinter, and J.A. Madri. 2000. Platelet-endothelial cell adhesion molecule (CD31), a scaffolding molecule for selected catenin family members whose binding is mediated by different tyrosine and serine/threonine phosphorylation. *J. Biol. Chem.* 275:21435–21443.

Ilan, N., L. Cheung, S. Miller, A. Mohsenin, A. Tucker, and J.A. Madri. 2001. PECAM-1 is a modulator of stat family member phosphorylation and localization: lessons from a transgenic mouse. *Dev. Biol.* 232:219–232.

Kalra, V.K., Y. Shen, C. Sultana, and V. Rattan. 1996. Hypoxia induces PECAM-1 phosphorylation and transendothelial migration of monocytes. *Am. J. Physiol.* 271:H2025–H2034.

Krug, E.L., R.B. Runyan, and R.R. Markwald. 1985. Protein extracts from early embryonic hearts initiate cardiac endothelial cytodifferentiation. *Dev. Biol.* 112:414–426.

Krug, E.L., C.H. Mjaatvedt, and R.R. Markwald. 1987. Extracellular matrix from embryonic myocardium elicits an early morphogenetic event in cardiac endothelial differentiation. *Dev. Biol.* 120:348–355.

Lee, K.F., H. Simon, H. Chen, B. Bates, M.C. Hung, and C. Hauser. 1995. Requirement for neuregulin receptor erbB2 in neural and cardiac development. *Nature.* 378:394–398.

Llorens, A., I. Rodrigo, L. Lopez-Barcons, M. Gonzalez-Garrigues, E. Lozano, A. Vinyals, M. Quintanilla, A. Cano, and A. Fabra. 1998. Down-regulation of E-cadherin in mouse skin carcinoma cells enhances a migratory and invasive phenotype linked to matrix metalloproteinase-9 gelatinase expression. *Lab. Invest.* 78:1131–1142.

Loffredo, C.A., P.D. Wilson, and C. Ferencz. 2001. Maternal diabetes: an independent risk factor for major cardiovascular malformations with increased mortality of affected infants. *Teratology.* 64:98–106.

Lu, T.T., L.G. Yan, and J.A. Madri. 1996. Integrin engagement mediates tyrosine dephosphorylation on platelet-endothelial cell adhesion molecule 1. *Proc. Natl. Acad. Sci. USA.* 93:11808–11813.

Lu, T.T., M. Barreuther, S. Davis, and J.A. Madri. 1997. Platelet endothelial cell adhesion molecule-1 is phosphorylatable by c-Src, binds Src-Src homology 2 domain, and exhibits immunoreceptor tyrosine-based activation motif-like properties. *J. Biol. Chem.* 272:14442–14446.

Mahooti, S., D. Graesser, S. Patil, P. Newman, G. Duncan, T. Mak, and J.A. Madri. 2000. PECAM-1 (CD31) expression modulates bleeding time in vivo. *Am. J. Pathol.* 157:75–81.

Miquerol, L., M. Gertsenstein, K. Harpal, J. Rossant, and A. Nagy. 1999. Multiple developmental roles of VEGF suggested by a LacZ-tagged allele. *Dev. Biol.* 212:307–322.

Miquerol, L., B.L. Langille, and A. Nagy. 2000. Embryonic development is disrupted by modest increases in vascular endothelial growth factor gene expression. *Development.* 127:3941–3946.

Mjaatvedt, C.H., and R.R. Markwald. 1989. Induction of an epithelial-mesenchymal transition by an in vivo adheron-like complex. *Dev. Biol.* 136:118–128.

Nakajima, Y., V. Mironov, T. Yamagishi, H. Nakamura, and R.R. Markwald. 1997. Expression of smooth muscle alpha-actin in mesenchymal cells during formation of avian endocardial cushion tissue: a role for transforming growth factor beta3. *Dev. Dyn.* 209:296–309.

Nakajima, Y., T. Yamagishi, S. Hokari, and H. Nakamura. 2000. Mechanisms involved in valvuloseptal endocardial cushion formation in early cardiogenesis: roles of transforming growth factor (TGF)-beta and bone morphogenetic protein (BMP). *Anat. Rec.* 258:119–127.

Natarajan, R., W. Bai, L. Lanting, N. Gonzales, and J. Nadler. 1997. Effects of high glucose on vascular endothelial growth factor expression in vascular smooth muscle cells. *Am. J. Physiol.* 273:H2224–H2231.

Newman, P.J. 1997. The biology of PECAM-1. *J. Clin. Invest.* 99:3–8.

Pinter, E., M. Barreuther, T. Lu, B.A. Imhof, and J.A. Madri. 1997. Platelet-endothelial cell adhesion molecule-1 (PECAM-1/CD31) tyrosine phosphorylation state changes during vasculogenesis in the murine conceptus. *Am. J. Pathol.* 150:1523–1530.

Pinter, E., S. Mahooti, Y. Wang, B.A. Imhof, and J.A. Madri. 1999. Hyperglycemia-induced vasculopathy in the murine vitelline vasculature: correlation with PECAM-1/CD31 tyrosine phosphorylation state. *Am. J. Pathol.* 154:1367–1379.

Pinter, E., J. Haigh, A. Nagy, and J.A. Madri. 2001. Hyperglycemia-induced vasculopathy in the murine conceptus is mediated via reductions of VEGF-A expression and VEGF receptor activation. *Am. J. Pathol.* 158:1199–1206.

Ramsdell, A.F., and R.R. Markwald. 1997. Induction of endocardial cushion tissue in the avian heart is regulated, in part, by TGFbeta-3-mediated autocrine signaling. *Dev. Biol.* 188:64–74.

Rattan, V., Y. Shen, C. Sultana, D. Kumar, and V.K. Kalra. 1996. Glucose-induced transmigration of monocytes is linked to phosphorylation of PECAM-1 in cultured endothelial cells. *Am. J. Physiol.* 271:E711–E717.

Rattan, V., C. Sultana, Y. Shen, and V.K. Kalra. 1997. Oxidant stress-induced transendothelial migration of monocytes is linked to phosphorylation of PECAM-1. *Am. J. Physiol.* 273:E453–E461.

Runyan, R.B., and R.R. Markwald. 1983. Invasion of mesenchyme into three-dimensional collagen gels: a regional and temporal analysis of interaction in embryonic heart tissue. *Dev. Biol.* 95:108–114.

Schimmenti, L.A., H.C. Yan, J.A. Madri, and S.M. Albelda. 1992. Platelet endothelial cell adhesion molecule, PECAM-1, modulates cell migration. *J. Cell. Physiol.* 153:417–428.

Song, W., K. Jackson, and P.G. McGuire. 2000. Degradation of type IV collagen by matrix metalloproteinases is an important step in the epithelial-mesenchymal transformation of the endocardial cushions. *Dev. Biol.* 227:606–617.

van Bruggen, N., H. Thibodeaux, J.T. Palmer, W.P. Lee, L. Fu, B. Cairns, D. Tumas, R. Gerlai, S.P. Williams, M. van Lookeren Campagne, and N. Ferrara. 1999. VEGF antagonism reduces edema formation and tissue damage after ischemia/reperfusion injury in the mouse brain. *J. Clin. Invest.* 104:1613–1620.

Wong, C.W., G. Wiedle, C. Ballestrem, B. Wehrle-Haller, S. Etteldorf, M. Bruckner, B. Engelhardt, R.H. Gisler, and B.A. Imhof. 2000. PECAM-1/CD31 trans-homophilic binding at the intercellular junctions is independent of its cytoplasmic domain; evidence for heterophilic interaction with integrin alphavbeta3 in Cis. *Mol. Biol. Cell.* 11:3109–3121.